

Thermodynamic Functions of Conformational Changes: Conformational Network of Glycine Diamide Folding, Entropy Lowering, and Informational Accumulation

Szilard N. Fejer,^{†,‡} Imre G. Csizmadia,^{†,§} and Bela Viskolcz^{*,†}

Department of Chemistry and Chemical Informatics, Faculty of Education, University of Szeged, P.O. Box 396, Szeged, Hungary 6701, University Chemical Laboratories, Cambridge CB2 1EW, United Kingdom, Department of Chemistry, University of Toronto, 80 St. George Street, Toronto, ON, Canada M5S 3H6

Received: August 29, 2006; In Final Form: October 2, 2006

A refined grid of a conformational potential energy surface (PES) and a conformational entropy surface for glycine diamide was generated by *ab initio* molecular computations. The possible network of reaction paths was recognized in terms of the linear combinations of internal coordinates corresponding to conrotatory and disrotatory modes of motions. Such a Woodward–Hoffmann-like path selection principle was detected for the folding of this peptide from extended to some virtually cyclic structure. It seemed reasonable to assume that this principle (or its generalized form) might be applicable to protein folding. A reaction path network was projected on the potential energy, and a continuous entropy surface was constructed under the condition of reduced dimensionality. The low entropy of the folded conformation indicated an information accumulation between 326% and 1414% with respect to the fully extended or unfolded structure. It is found that the location of existing and ‘latent’ critical points on the surface is revealed by the extrema and inflection points of the entropy curve.

Introduction

On the conformational potential energy functions of hydrocarbons¹ or simple substituted hydrocarbons² the reaction paths are close to the unperturbed motions of single rotors. However, geminal substituents very often interact extensively. For example, vibrational modes could be coupled into symmetric and asymmetric modes. Also, their internal rotations may be coupled into conrotatory and disrotatory modes as illustrated in the upper part of Figure 1. If the geminal substituents are identical (i.e., $Z_1 = Z_2$), then the conrotatory path involves the vectorial sum ($\psi + \phi$) and the disrotatory path involves the vectorial difference ($\psi - \phi$) of the basis vectors of internal rotations: ψ and ϕ (Figure 1 central part). These combined modes of internal rotations also play an important role in describing the thermal intramolecular rearrangements of pericyclic reactions, as specified by the Woodward–Hoffmann selection rule.³ Accordingly, $4n$ π -electron systems are allowed to undergo thermal electrocyclic reactions *via* a conrotatory mode of motion, while $4n + 2\pi$ -electron systems are allowed to proceed, thermally, through low barriers *via* a disrotatory mode of motion.^{4,5}

If the two functional groups, denoted by Z_1 and Z_2 (Figure 1), are not identical, the conrotatory and disrotatory linear combinations are somewhat distorted. This is the case for peptide residues such as glycine diamide (central part of Figure 1). The conformational PES of glycine diamide exhibits five stable conformers out of the possible nine structures as shown in the lower part of Figure 1. Thus, in accordance with the lower part of Figure 1, the β , γ , and δ conformers are manifested minima. In contrast to that, the α and ϵ folded structures, which do occur

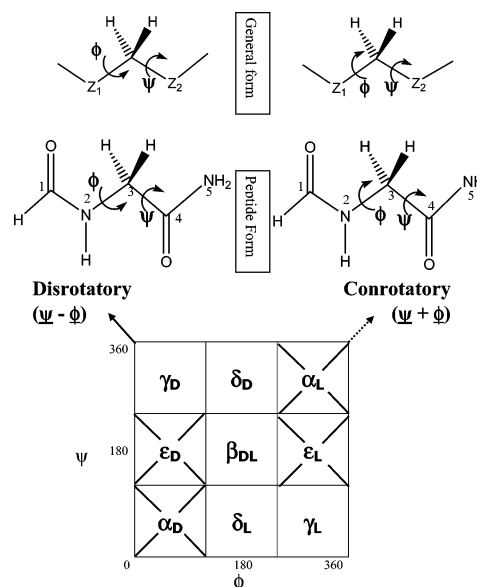


Figure 1. Top: The conrotatory and disrotatory modes of motions for molecules containing a geminally substituted carbon atom. The directions of conrotatory and disrotatory modes of motions are clearly indicated. Bottom: Topology of the PES of peptide diamide conformations. The conrotatory and disrotatory modes of motions for glycine diamide are clearly indicated as linear combinations of $\phi(1,2,3,4)$ and $\psi(2,3,4,5)$.

in folded proteins are only ‘latent’ minima here, since they are not manifested on the PES at this level of theory.

It might be of casual interest to look, at least *per tangentem*, into the rather loose analogy that may exist between the pericyclic ring closure and the folding of the extended form β_{DL} of the simplest peptide (lower part of Figure 1) into its hydrogen-bonded cyclic conformers (γ_L and γ_D). In accordance with the Woodward–Hoffmann rule, 10π -electron conjugated

* To whom correspondence should be addressed. E-mail: viskolcz@jgyt.f.u-szeged.hu.

[†] University of Szeged.

[‡] University Chemical Laboratories.

[§] University of Toronto.

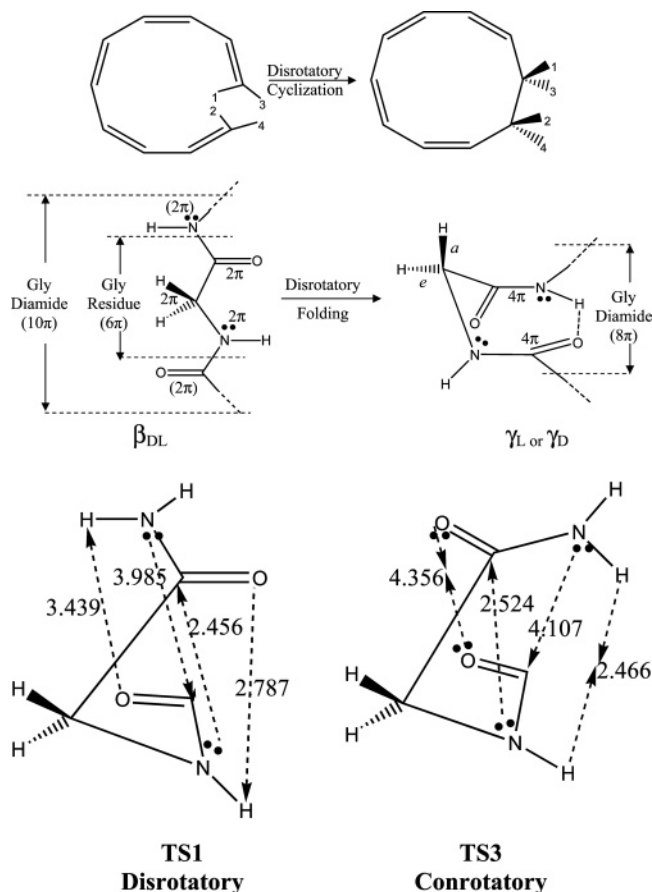


Figure 2. Woodward-Hoffmann principle for an electrocyclic reaction of glycine diamide folding. The Gly residue contains six π -electrons, and with the associated peptide bonds it contains 10 π -electrons. Both of them correspond to a $(4n + 2)$ π -electron system. After the cyclization reactions, the 10 π conjugated electrons are converted to two non-overlapping 4 π -electron systems.

systems may undergo thermal cyclization *via* the disrotatory mode of motion with a low barrier height. One pair of π -electrons is removed from the system during the ring closure process; thus, eight π -electrons remain conjugated. A σ -bond is formed during the ring closure (Figure 2 top). The analogy of the previously stated Woodward-Hoffmann selection rule for the peptide folding process suggests that due to the hyperconjugative interaction of the CH_2 moiety, in the extended or β_{DL} conformation, glycine diamide may be regarded to contain 10 (i.e., $4n + 2$) π -electrons (central part of Figure 2). The low barrier of folding is along the disrotatory mode of motion, which converts the extended chain, β_{DL} , to a cyclic structure, γ_{L} or γ_{D} (i.e., $\text{g}^- \text{g}^+ \leftarrow \text{aa} \rightarrow \text{g}^+ \text{g}^-$), held together in a cyclic form by an intramolecular hydrogen bond. In this cyclic structure the CH_2 moiety is out of plane; therefore, two π -electrons are removed from the system since hyperconjugation is not possible anymore. Thus, these conformers have two sets of four π -electrons which are not in a conjugative relationship although they may interact to a small extent through space *via* the hydrogen-bonded ring closure.

Thus, the analogy amounts to nothing more than that a $(4n + 2) = 10$ π -electron-containing α -peptide unit is folded preferentially (i.e. *via* lower conformational barrier) along the disrotatory mode, while the conrotatory mode had a somewhat higher barrier. It might be of passing interest to note that β -peptides, $\text{H}-\text{CH}_2-\text{CH}_2-\text{CONH}-$ (consisting of not 10 but 12 π -electrons per peptide residue), seemed to be folded preferentially along a nearly conrotatory path on the 3D potential

TABLE 1: Geometrical Parameters of Zeroth- and First-Order Critical Points of Glycine Diamide PES^a

	φ	ψ	ω_0	ω_1	$R_{\text{N-H}\cdots\text{O}}$
β_{DL}	180.00	180.00	180.00	180.00	5.16
γ_{D}	80.34	-68.67	178.12	174.76	2.06
γ_{L}	-80.34	68.67	-178.12	-174.76	2.06
δ_{D}	119.64	-20.42	174.27	-169.71	3.53
δ_{L}	-119.64	20.42	-174.27	169.71	3.53
TS1 _D	94.73	-123.37	-172.56	172.63	3.44
TS1 _L	-94.73	123.37	172.56	-172.63	3.44
TS2 _D = TS2 _L	0.00	0.00	180.00	180.00	1.77
TS3 _D	49.34	111.25	171.41	-177.99	4.98
TS3 _L	-111.25	-49.34	-171.41	177.99	4.98
TS4 _D	110.63	-25.54	175.56	-168.76	3.23
TS4 _L	-110.63	25.54	-175.56	168.76	3.23

^a Angles in degrees; distances in angstroms.

energy hypersurface: $E = f(\varphi, \mu, \psi)$. Corresponding to the idealized conrotatory direction of $\{\text{g}^+[\text{g}^+]\text{g}^+\} \leftarrow \{\text{a}[\text{a}]\text{a}\} \rightarrow \{\text{g}^-[\text{g}^-]\text{g}^-\}$, a somewhat distorted path, but with a general conrotatory direction, on a 2D cross-section of the hypersurface has been exemplified recently.⁶

It has been shown, in a previous publication,⁷ that in the case of the conformational change in *n*-butane, the entropy calculated in the $3N - 7$ reduced dimensionality was lowered systematically from *anti* to *gauche* to *syn* conformations. This entropy lowering corresponded to an information accumulation of 16% and 42%, respectively. If the van der Waals interaction of two methyl groups resulted in such a noticeable information accumulation, one may assume that peptide folding will show a considerably larger change. The present paper examines the folding of glycine diamide from this point of view.

The potential energy surface (PES) of glycine diamide has been studied previously.⁸⁻¹¹ However, the conformational network on thermodynamic surfaces has never been explored.

Methods

According to the method described previously,^{7,12} the normal coordinate analyses for each geometry were carried out involving all internal coordinates, which were at their minima, except the internal rotation about the $\text{N}-\text{C}^\alpha$ (ϕ) and $\text{C}^\alpha-\text{CO}$ (ψ) bonds.

All G3MP2B3¹³ computations were carried out with the Gaussian-03 program package¹⁴ under tight optimization conditions. The ϕ and ψ dihedral angles were varied in 10° steps to construct the continuous energy and entropy surfaces. Consequently, these surfaces were computed at a reduced dimensionality, containing $3N - 8$ internal degrees of freedom. At the energy minima and at the first-order saddle points, the thermodynamic functions were also calculated classically, with $3N - 6$ and $3N - 7$ internal degrees of freedom, respectively. Using IRC^{15,16} calculations starting from the transition states found on the surface, a network of the paths was established, which connects the corresponding 0th and first order critical points with each other.

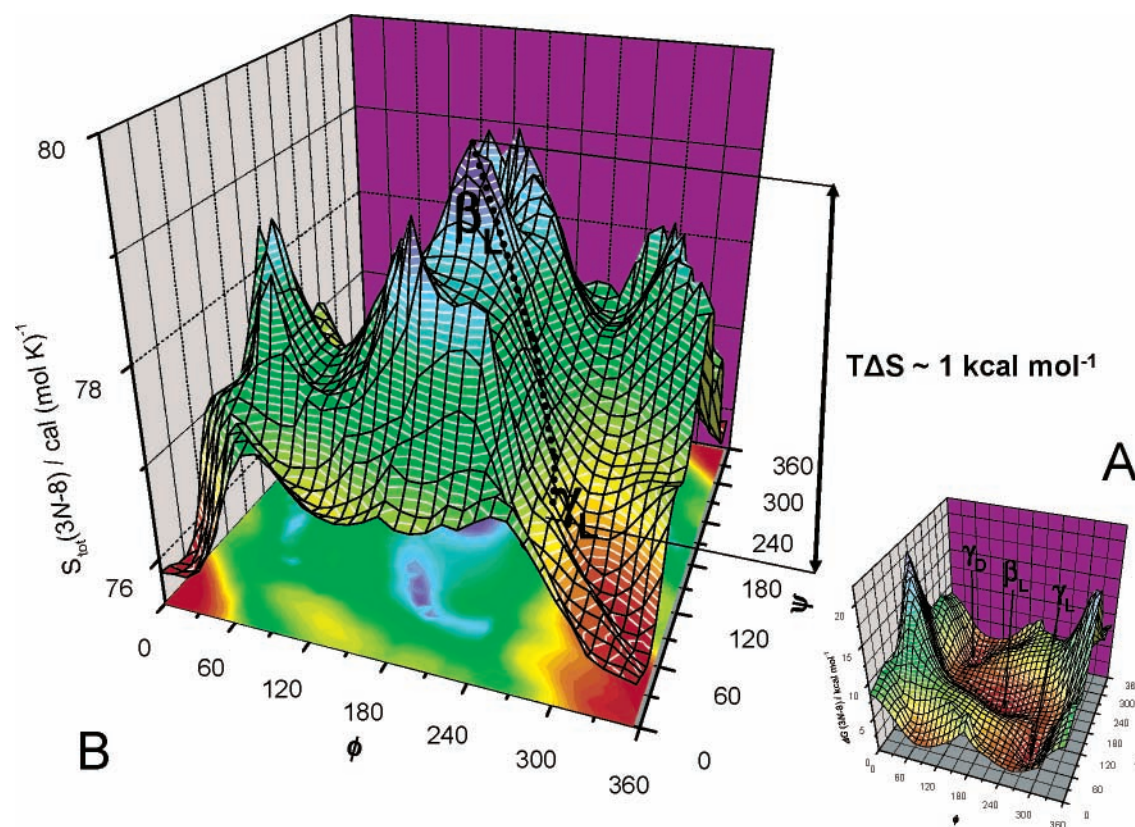
Results and Discussion

The optimized geometrical parameters for the 0th and first order critical points are summarized in Table 1. The $\text{N}\cdots\text{H}-\text{O}$ atom distance indicates the strength¹⁷ of the intramolecular interaction during the rotational motion. The computed thermodynamic functions (Table 2) for the various critical points of the conformational PES of glycine diamide are strongly dependent on this interaction. Three-dimensional representations of the Ramachandran type potential energy surface and associated entropy surface for the conformational folding of glycine

TABLE 2: Relative Energies, Enthalpies, and Free Energies (in kcal mol⁻¹), Absolute as Well as Relative Entropies (in cal mol⁻¹K⁻¹), and Relative Informational (I_{rel}) Content for the Glycine Folding of Selected Characteristic Points of Conformational Changes, Taking into Account $3N - 6$ and $3N - 8$ Degrees of Freedom, Respectively

conf ^a	ΔE	ΔH ($3N - 6$)	ΔH ($3N - 8$)	ΔG ($3N - 6$)	ΔG ($3N - 8$)	S_{tot} ($3N - 6$)	S_{tot} ($3N - 7$)	S_{tot} ($3N - 8$)	ΔS ($3N - 6$)	ΔS^\ddagger	ΔS ($3N - 8$)	$I_{rel} = I_x/I_B$ ($3N - 8$)
β_{DL}	0.00	0.00	0.00	0.00	0.00	89.698	—	79.58 5	0.00	—	0.00	1.00
TS1 ^b	2.04	1.87	2.47	4.13	3.23	—	82.112	77.01 2	—	-7.59	-2.57	3.66
γ_L	-0.50	-0.03	-0.05	1.58	0.81	84.316	—	76.71 5	-5.38	—	-2.87	4.26
TS2 ^b	5.76	5.68	6.27	7.91	7.36	—	82.191	75.92 4	—	-7.51	-3.66	6.35
γ_D	-0.50	-0.03	-0.05	1.58	0.81	84.316	—	76.71 5	-5.38	—	-2.87	4.26
TS4 ^b	2.04	1.68	2.27	3.99	2.91	—	81.94	77.43 2	—	-7.76	-2.15	2.96
δ_D	2.01	2.23	2.23	2.97	2.86	87.221	—	77.45	-2.48	—	-2.13	2.93
TS3 ^b	7.26	6.70	7.29	8.42	7.53	—	83.905	78.77 9	—	-5.79	-0.80	1.50
β_{DL}	0.00	0.00	0.00	0.00	0.00	89.698	—	79.58 5	0.00	—	0.00	1.00

^a Since the α -carbon of glycine is a prochiral center, therefore, the $\gamma_L = \gamma_D$ and $\delta_L = \delta_D$ degeneracy is observed. ^b For TSs instead of $3N - 6$, $3N - 7$ internal coordinates were used. For TS1 and TS2 the omitted coordinate was taken along the disrotatory mode of motion, and for TS3 and TS4 the omitted coordinate was along the conrotatory mode of motion; these modes with imaginary frequencies correspond to the reaction coordinate according to the transition state theory. For consistency, all values shown are calculated with the B3LYP/6-31G(d) level of theory. The G3MP2B3 energy results do not alter the overall trends.

**Figure 3.** Three-dimensional representations of the Ramachandran type potential energy surface (A) and associated entropy surface (B) for the conformational folding of glycine diamide as functions of ϕ and ψ .

diamide are shown in Figure 3A and Figure 3B, respectively. All 0th and first order critical points found are shown on the PES associated with the folding of glycine diamide (Figure 4A). The square of solid lines at the lower left-hand side shows the IUPAC cut of the Ramachandran PES from -180° to $+180^\circ$ along both ϕ and ψ . The broken line square, covering the area from 0° to $+360^\circ$ along both ϕ and ψ , represents the traditional cut of the Ramachandran map. The network of conformational changes clearly involves virtually infinite long major paths along the disrotatory mode of motion placed in every 360° in a nearly parallel fashion. In contrast to that, along the conrotatory direction, a path only connects three adjacent disrotatory paths. Thus, folding along the conrotatory mode of motion for an infinitely long path must involve the utilization of a short distance ($\beta_{DL} \rightarrow \gamma_L$ or $\beta_{DL} \rightarrow \gamma_D$) along the disrotatory path.

Such an arrangement leads to “Enantiotopic Reaction Coordinates” (Figure 5). On the basis of the reaction kinetic principle, in a multistep reaction the lower barrier must precede the higher barrier along the reaction coordinate for a kinetically favored mechanism. These enantiotopic energy profiles are shown at the left- and right-hand side of Figure 5.

Figure 4B shows the entropy surface of glycine diamide. The network marked on this map is the same as that used in Figure 4A. Viewing along the various paths of the network one can see the entropy change associated with the various conformational changes.

In a very general sense, the entropy surface illustrates the extent of any attractive or repulsive intramolecular interactions. Such interactions alter the vibrational state of the molecule, which in turn results in altered intrinsic entropy. According to

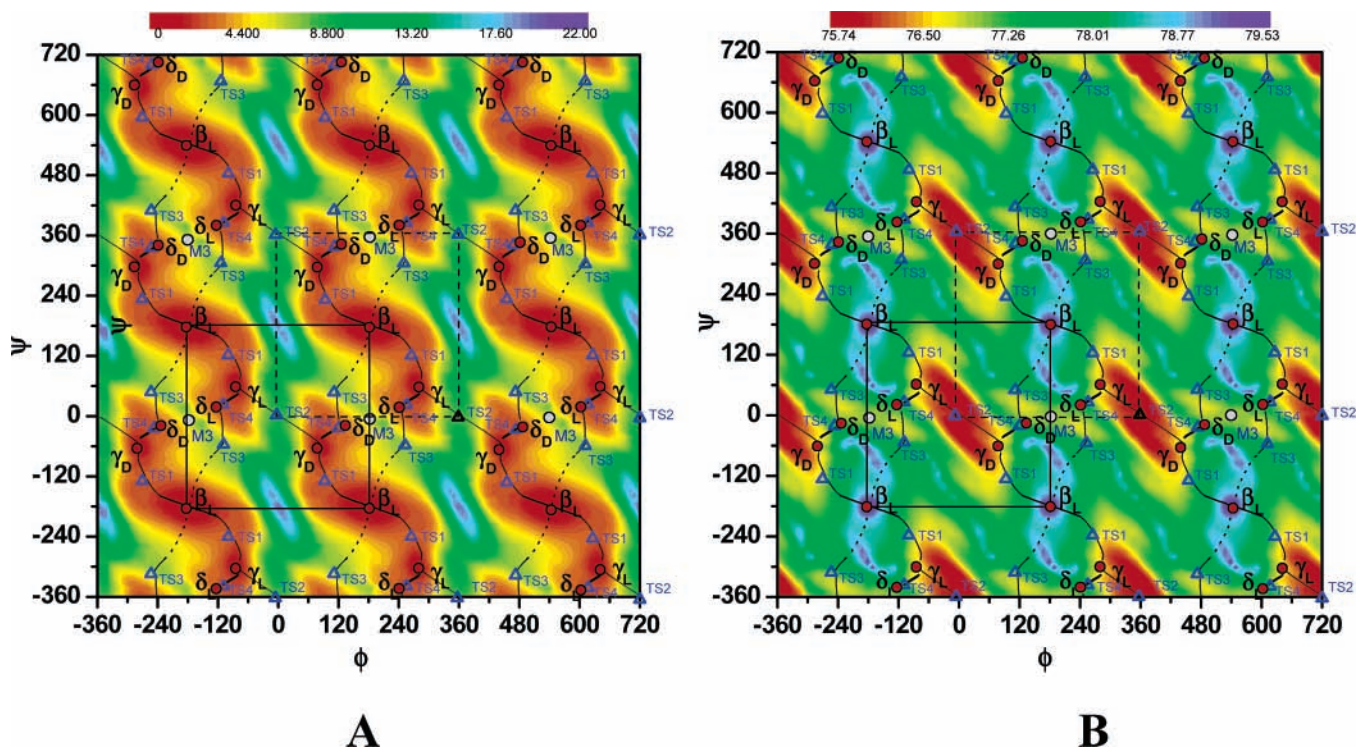


Figure 4. (A) Potential energy surface (in kcal mol⁻¹) of glycine diamide. The solid square at the lower left-hand side represents the IUPAC recommended cut from -180° to $+180^\circ$ of both ϕ and ψ . The broken square at the center represents the traditional cut from 0 to 360 of both ϕ and ψ . (B) Entropy surface [in cal (mol K)⁻¹] of glycine diamide computed for $3N - 8$ degrees of freedom.

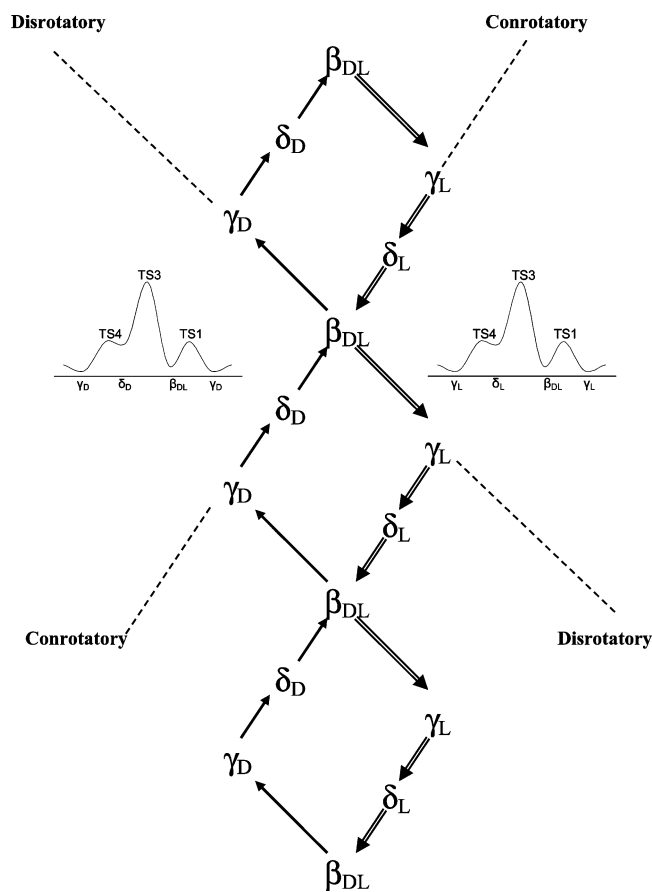


Figure 5. "Hysteresis loops" or "enantiotopic reaction coordinates" for the forward and reverse reaction paths along the conrotatory mode of motion.

the topology of the entropy surface, stronger attractive or repulsive interactions result in a lower intrinsic entropy.

In order to see the energy as well as entropy change along the folding routes it is necessary to plot these quantities along the conrotatory and disrotatory reaction coordinates. In both of these two reaction coordinates the central point is the β_{DL} conformer, as these two paths cross each other at that geometry ($\phi = 180^\circ$ and $\psi = 180^\circ$). Such plots are shown in Figure 6. The two energy profiles clearly indicate that the barriers are lower along the disrotatory path than along the conrotatory path ((A) and (B) of Figure 6). The two entropy profiles ((C) and (D) in Figure 6) are directly underneath the energy profiles. This arrangement makes it possible to compare the location of the critical points on the energy profile with the location of the critical points on the entropy profile.

From (A) and (B) of Figure 6, one can see that the β - γ transition (TS1) is thermodynamically favored along the disrotatory mode of motion, and the energy barriers along the conrotatory mode of motion are considerably higher (TS3). The geometries of TS1 and TS3 are shown schematically in Figure 2 (lower part). Interestingly, the favored path has a much 'smoother' entropy profile than the conrotatory path as shown in C and D of Figure 6. Along the disrotatory path, starting from the β_{DL} conformer, the intrinsic entropy of the molecule decreases more or less monotonically all the way to the vicinity of the γ conformer.

It should be noted that the energy difference between the unfolded β_{DL} and folded γ_L and γ_D conformation is relatively small (-0.5 kcal/mol). In contrast to that, the entropy difference between the unfolded (β_{DL}) and folded (γ_L and γ_D) structures is relatively large (almost 3 entropy units) even on the reduced $3N - 8$ internal coordinates and considerably larger (over 5 entropy units) on the full $3N - 6$ freedom of motion. This implies that relative energy hides, at least to some degree, while entropy reveals the extent of folding in a more pronounced way. In other words, while the energy change cannot, the intrinsic

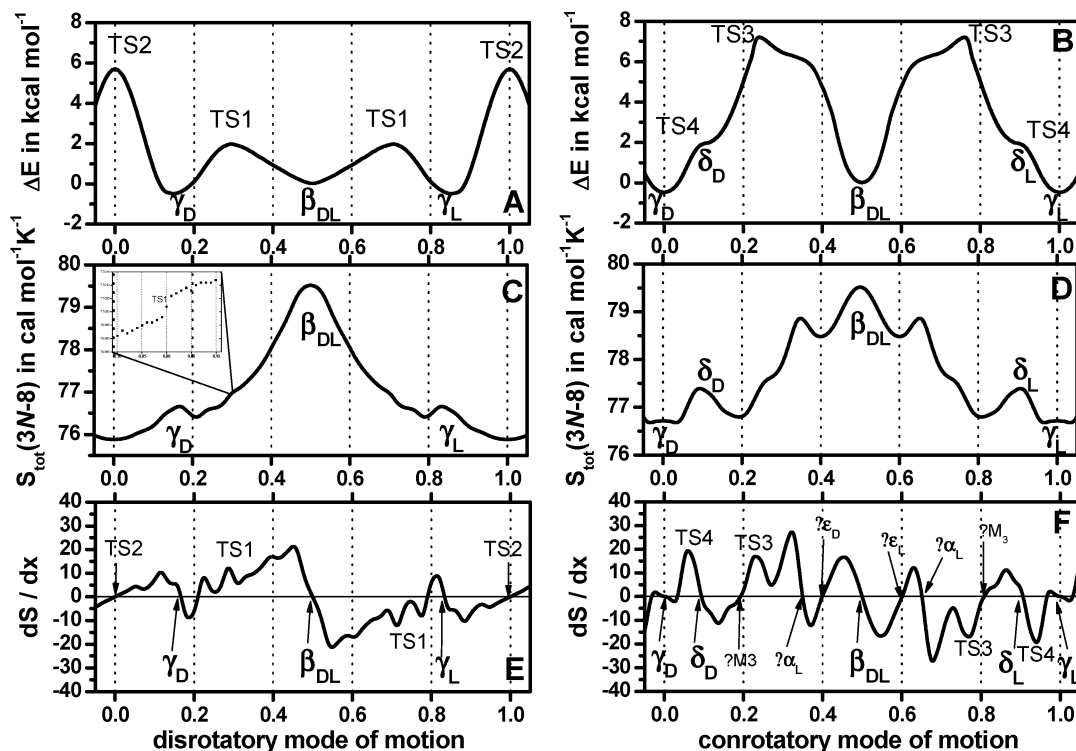


Figure 6. Energy and entropy variations along the conrotatory and disrotatory modes of motion (left column is the conrotatory, right column is the disrotatory mode). (A) and (B) are energy, (C) and (D) are entropy, (E) and (F) are the derivative of entropy.

entropy change can, in fact, be used as a diagnostic measure of the extent of folding.

The computed relative entropy can be used to calculate the information content (I_x) of a given conformation (x) as the multiple of the information content (I_β) of the reference conformation: β_{DL}

$$I_x = I_\beta \exp(-\Delta S/R) \quad \text{or} \quad \ln \left[\frac{I_x}{I_\beta} \right] = \left[-\frac{1}{R} \right] \Delta S \quad (1)$$

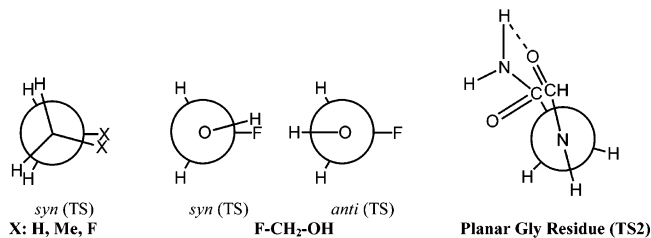
These values, calculated for the $3N - 8$ reduced dimensionality, are summarized in the last column of Table 2. It is noteworthy that the γ_L and γ_D conformers have

$$100(4.26 - 1.00) = 326\% \quad (2)$$

more information than the reference β_{DL} conformer. Similar calculations can be made on the full dimensionality of $3N - 6$. In that case the γ_L and γ_D conformers have 1414% more information than the reference β_{DL} conformer. This information accumulation is caused by the formation of a ring-like structure, shown in Figure 2. Clearly, the hydrogen bonding in the γ_L and γ_D conformations, which leads to a cyclic structure, lowers the entropy substantially. This in turn means an accumulation of a considerably larger amount of information than the weak van der Waals interaction of two methyl groups in the *syn* arrangement in *n*-butane.⁷ The variation of the log of relative information, $\ln[I_x/I_\beta]$, with respect to ΔS is shown in Figure 7 for glycine diamide as well as other simple organic compounds specified in Scheme 1.

It has been found previously^{7,12} that the entropy function has a maximum where the energy function is at its minimum and the energy transition states turned out to be close to entropy minima in the case of these simple compounds. For the glycine diamide, most of the maxima of the entropy curves along the reaction path network are found in the close vicinity of the β_{DL} , γ_L , γ_D , δ_L , and δ_D stable conformers, as may be seen as we

SCHEME 1



compare (A) with (C) and (B) with (D) in Figure 6. In contrast to this, it is not immediately obvious in the case of glycine diamide what the specific appearance of the transition states of the energy profiles ((A) and (B) of Figure 6) would be in the entropy profiles ((C) and (D) of Figure 6). The small inset in (C) suggests that the actual nonsymmetric energy transition states are manifested as inflection points on the entropy function. The only exception to that rule is TS2 where point symmetry, and the continuation of the dS/dx function along the periodic disrotatory mode, demands that $dS/dx = 0$. In fact previous experience suggests that for symmetric transition states of the energy profile, the entropy profile has a minimum value, so its derivative would be zero as exemplified in Scheme 1.

In this way, all existing minima and transition states may be identified on the (dS/dx) functions ((E), and (F) in Figure 6). Another interesting critical point labeled as M3 was found on the PES, which is expected to have (dS/dx) = 0 by symmetry. This third-order critical point with three imaginary frequencies ($445i$, $112i$, and $29i$ cm^{-1}) is in an energy maximum along three internal coordinates. However, only one of the three is related to the conformational space $\{\phi, \psi\}$; the other two motions are related to the pyramidal inversion of the N-atoms. This point seems to be a crossing between two surfaces of different electronic states.¹⁸ No reaction path is associated with this critical point. In (F) of Figure 6 the crossings of the x -axis along

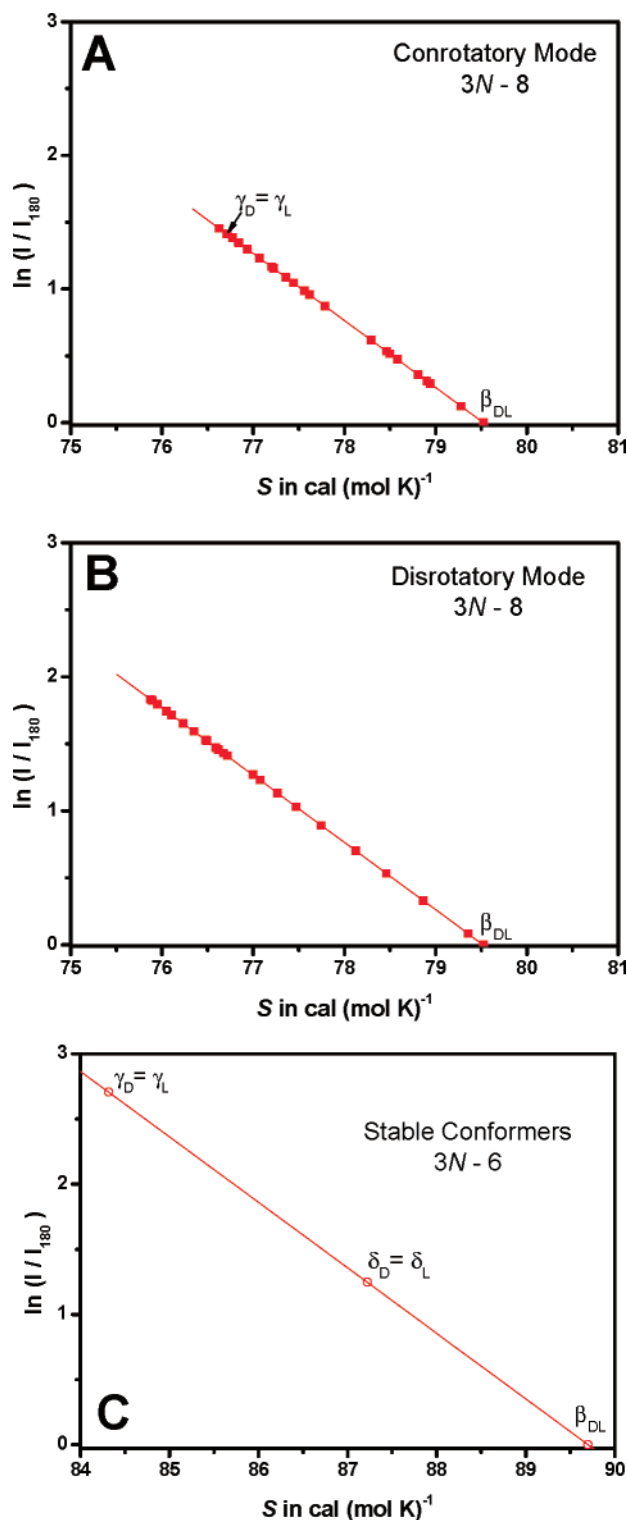


Figure 7. Relative information content of glycine diamide conformations: (A) along the conrotatory mode, (B) disrotatory mode, (C) optimized stable conformers.

the reaction coordinate for M3 appear to be at about 0.2 and 0.8.

The change in curvature of the PES is changing the vibrations, which define the intrinsic entropy (S) of the molecule. Consequently, the derivative (dS/dx) helps us to locate these changes and therefore the “manifested” minima and transition states. Even higher order critical points may be easily identified on the (dS/dx) function. However, it appears that the critical points not manifested on the PES may also show up on the (dS/dx)

function. These might be called “latent” critical points in agreement with an earlier observation¹⁹ in the case of $\text{FCH}_2\text{-OH}$. Some of these nonmanifested conformers, namely α_L , α_D , ϵ_L , ϵ_D , as well as an approximate location for M3 have been identified in (E) and (F) of Figure 6.

All in all, it appears that the entropy surface, or its equivalent information surface calculated according to eq 1, keeps all the information of the potential energy surface topology. In other words, all the information is present, permanently, about all minima and transition states, irrespective of whether they are latent or manifested, and these may be observed on the entropy surface cross-sections along the paths of conformational changes which are forming a network on the PES. Perhaps, this new observation may be important in the process of deciphering the law that governs protein folding.

Conclusion

After the position of the minima and transitions on the conformational potential energy surface (PES) has been determined, paths for conformational changes emerged. The computed energy values revealed that along the disrotatory mode of motion the barrier heights are lower than along the conrotatory path. This suggests a Woodward–Hoffmann-like principle in path selection of thermal conformational changes for the $4n + 2 = 10$ π -electron system of glycine diamide.

The continuous entropy surface $S(\phi, \psi)$ on the whole PES was calculated using reduced dimensionality ($3N - 8$) since ψ and ϕ were fixed at each of the grid points. We have shown that the 3D entropy surface is an excellent diagnostic tool for the analysis of the folding even of such a small system as glycine diamide. It is also shown that the entropy surface, when combined with the possible reaction paths from the underlying PES, holds information about the location of manifested minima and transition states on the surface, and it is assumed that these entropy curves also show the approximate location of ‘latent’ minima and transition states, which may be manifested for example in larger peptide conformations.

According to the topology of the continuous entropy surface, substantial information accumulation was detected for the folded conformers compared to the stretched β_{DL} structure. The folded structure can hold more than 4 times more information as the unfolded one. This can be interpreted as structural information showing the extent of intramolecular interactions. It remains to be seen to what extent information accumulation plays an important role for the folding of all biopolymers such as proteins, RNA, and DNA.

Acknowledgment. I.G.C. thanks the Ministry of Education for a Szent-Györgyi Visiting Professorship. The authors are grateful to the Hungarian Scientific Research Fund for financial support (OTKA T046861 and F037648). V.B. thanks the National Office for Research and Technology for an Öveges Research Program (HEF_06_1-PESINF06).

Supporting Information Available: The Supporting Information for this paper consists of important geometry parameters of the found 0th and first-order critical points on the surface, as well as their vibrational frequencies. This information is available free of charge via Internet at <http://pubs.acs.org>.

References and Notes

- (1) Peterson, M. R.; Csizmadia, I. G. *J. Am. Chem. Soc.* **1978**, *100*, 6911.

- (2) Kehoe, T. A. K.; Peterson, M. R.; Chass, G. A.; Viskolcz, B.; Stacho, L.; Csizmadia, I. G. *J. Mol. Struct. (THEOCHEM)* **2003**, *79*, 666–667.
- (3) Hoffmann, R.; Woodward, R. B. *J. Am. Chem. Soc.* **1965**, *87*, 395.
- (4) Woodward, R. B.; Hoffmann, R. *The Conservation of Orbital Symmetry*; Verlag Chemie: Weinheim, 1970.
- (5) Longuet-Higgins, H. C.; Abrahamson, E. W. *J. Am. Chem. Soc.* **1965**, *87*, 2045.
- (6) Beke, T.; Czajlik, A.; Csizmadia, I. G.; Perczel, A. *Phys. Biol.* **2006**, *3*, 1–14. (see particularly Figure 3b).
- (7) Viskolcz, B.; Fejer, S. N.; Csizmadia, I. G. *J. Phys. Chem. A.* **2006**, *110* (10), 3808.
- (8) Head-Gordon, T.; Head-Gordon, M.; Frisch, M. J.; Brooks, C. L., III; Pople, J. A. *J. Am. Chem. Soc.* **1991**, *113*, 5989.
- (9) Perczel, A.; Angyan, J. G.; Kajtar, M.; Viviani, W.; Rivail, J. L.; Marcoccia, J. F.; Csizmadia, I. G. *J. Am. Chem. Soc.* **1991**, *113*, 6256.
- (10) McAllister, M. A.; Perczel, A.; Császár, P.; Viviani, W.; Rivail, J. L.; Csizmadia, I. G. *J. Mol. Struct. (THEOCHEM)* **1993**, *288*, 161.
- (11) Law, J. M. S.; Setiadi, D. H.; Chass, G. A.; Csizmadia, I. G.; Viskolcz, B. *J. Phys. Chem. A.* **2005**, *109*, 520.
- (12) Viskolcz, B.; Fejer, S. N.; Szori, M.; Csizmadia, I. G. *Mol. Phys.* **2006**, *104*, 795.
- (13) Curtiss, L. A.; Redfern, P. C.; Raghavachari, K.; Rassolov, V.; Pople, J. A. *J. Chem. Phys.* **1999**, *110*, 4703.
- (14) *Gaussian 03* package was used, as specified in Supporting Information.
- (15) Gonzalez, C.; Schlegel, H. B. *J. Chem. Phys.* **1989**, *90*, 2154.
- (16) Gonzalez, C.; Schlegel, H. B. *J. Phys. Chem.* **1990**, *94*, 5523.
- (17) Tang, T.-H.; Derety, E.; Knak Jensen, S. J.; Csizmadia, I. G. *Eur. Phys. J. D.* **2006**, *37*, 217.
- (18) Bunker, P. R.; Jensen, P. *Molecular Symmetry and Spectroscopy*, 2nd ed.; NRC Research Press: Ottawa, 1998.
- (19) Viskolcz, B.; Szori, M.; Izsak, R.; Fejer, Sz. N.; Csizmadia, I. G. *Int. Quantum Chem.*, submitted.